In situ monitoring of structure formation in the active layer of polymer solar cells during roll-to-roll coating

Rossander, Lea Hildebrandt; Zawacka, Natalia Klaudia; Dam, Henrik Friis; Krebs, Frederik C; Andreasen, Jens Wenzel

Published in:
A I P Advances

Link to article, DOI:
10.1063/1.4892526

Publication date:
2014

Document Version
Publisher's PDF, also known as Version of record

AIP Advances

In situ monitoring of structure formation in the active layer of polymer solar cells during roll-to-roll coating

Lea H. Rossander, Natalia K. Zawacka, Henrik F. Dam, Frederik C. Krebs, and Jens W. Andreasen

Citation: AIP Advances **4**, 087105 (2014); doi: 10.1063/1.4892526
View online: http://dx.doi.org/10.1063/1.4892526
View Table of Contents: http://scitation.aip.org/content/aip/journal/adva/4/8?ver=pdfcov
Published by the AIP Publishing

AIP ADVANCES **4**, 087105 (2014)

In situ monitoring of structure formation in the active layer of polymer solar cells during roll-to-roll coating

Lea H. Rossander, Natalia K. Zawacka, Henrik F. Dam, Frederik C. Krebs, and Jens W. Andreasen[a]
Department of Energy Conversion and Storage, Technical University of Denmark, Frederiksborgvej 399, DK-4000, Denmark

(Received 29 April 2014; accepted 25 July 2014; published online 5 August 2014)

The active layer crystallization during roll-to-roll coating of organic solar cells is studied *in situ*. We developed an X-ray setup where the coater unit is an integrated part of the small angle X-ray scattering instrument, making it possible to control the coating process while recording scattering measurements *in situ,* enabling us to follow the crystal formation during drying. By varying the distance between the coating head and the point where the X-ray beam hits the film, we obtained measurements of 4 different stages of drying. For each of those stages, the scattering from as long a foil as possible is summed together, with the distance from coating head to scattering point kept constant. The results are average crystallographic properties for the active layer coated on a 30 m long foil. With this insight into the dynamics of crystallization in a roll-coated polymer film, we find that the formation of textured and untextured crystallites seems uncorrelated, and happens at widely different rates. Untextured P3HT crystallites form later in the drying process than expected which may explain previous studies speculating that untextured crystallization depends on concentration. Textured crystallites, however, begin forming much earlier and steadily increases as the film dries, showing a development similar to other *in situ* studies of these materials. [http://dx.doi.org/10.1063/1.4892526]

I. INTRODUCTION

Solar energy will constitute an important, if not dominant, part of a future energy supply because of the large abundance – the total incoming power in sunlight at the Earth's surface is on the order of 100.000 TW. Compared to the estimated theoretical potential of wind and geothermal energy (around 15 TW), solar power is the only sustainable energy source with a potential to completely supply human consumption today, and by a large margin also our future needs that are projected to increase significantly. Since the first solar cells were realized in the 1950s they have been improved immensely, but still these 1st generation solar cells have shortcomings in the form of high processing cost and a required flat and solid form factor. Organic solar cells represent a possible improvement because they can be processed using roll-to-roll (R2R) processing; a well-known manufacturing technique used by the newspaper industry that present high printing speeds. This has inspired hope that solar cells could one day be manufactured in a similar fashion.[1] The challenge is to develop photoactive blends that produce efficient solar cells when printed, because the film forming process itself affects the efficiency of the cells.

The most promising kind of organic solar cells use a bulk heterojunction (BHJ), a mixture of two materials, one material being an electron donor (polymer) and the other an electron acceptor (e.g. fullerene).[2–4] Until today it is the most effective design because of the way electric current is

[a]Author to whom correspondence should be addressed. Electronic mail: jewa@dtu.dk

generated in an organic solar cell. In contrast to silicon solar cells, the electron-hole pair created by an incoming photon is strongly bound in a so-called exciton.[5,6] To enable utilization of the charge carriers, the exciton has to be dissociated, which happens at places where the energetic gain for the disassociated electron is larger than the binding energy of the exciton, for example at the interface of an electron donor and acceptor. The exciton has to reach such an interface before it recombines, giving the internal size parameters or morphology of the donor/acceptor mixture a high influence on the solar cell efficiency. The exciton lifetime sets a limit to the average diffusion length of about 10 nm, so if most of the created excitons are to reach an interface, the length scale of the fullerene-polymer phase segregation has to be less than 20 nm.[7] Most of the BHJ's used are self-assembling and in order to understand why some created structures are better than others, a wide range of imaging techniques are used to characterize the structure of the active layers, and thereby connect a specific morphology to the performance of the solar cell. About half[8] of the polymer/fullerene mixture forms semi-crystalline regions, which is possible to investigate using X-ray diffraction. Furthermore, X-rays are non-destructive to the polymers, and sensitive to the nanometer scale when using small scattering angles (SAXS). Therefore this technique has been used extensively to study BHJ layers, both individually and as a part of fully functional solar cells,[6] but until now R2R processed solar cells have only been studied *ex situ*.[9] Few requirements for special sample environments enable *in situ* studies of materials, and at the same time the X-ray measurements give a statistical average over the whole thickness of the film, important especially in the case of BHJ films because their inner morphology is the most important factor to determine.

P3HT crystallizes in various ways that have been reported in the litterature.[6] First, it often crystallizes in the plane of the interfaces with substrate and air, resulting in a distinct Bragg peak corresponding to the lamellar stack (*100*). The peak is seen in the out-of-plane or in-plane direction with respect to the interface, depending on the orientation of the polymer back bone – if it orients with the aromatic planes perpendicular to the interface we call it edge-on and the *100* Bragg peak appears out-of-plane, if it orients parallel to the interface shown by an in-plane *100* Bragg peak, it is called face-on.[10] Crystallites formed in the bulk material tend to scatter in random orientations between these extremes, forming a ring similar to a regular powder diffraction pattern because they exhibit all possible orientations. They are called untextured crystallites. The crystallites that show a preferential orientation are called textured crystallites. The conductivity and thereby efficiency of the solar cells have been shown to be improved both by the total amount of crystallinity[11] and higher amounts of face on oriented crystallites.[12]

The two other popular solution-based solar cell processing techniques, doctor blading[13] and spin coating,[14] have recently also been studied *in situ* using X-rays. Sanyal *et al.*[13] studied doctor-blading, and Chou *et al.*[14] studied spin coating, and both experiments found similar results, showing that textured edge-on crystallization begin first, followed by a gradual increase of the amount of untextured crystallites. In the case of doctor-bladed active layers, higher drying temperature results in more edge on textured crystallization, but less π-π packing and therefore lower solar cell efficiency. The results cannot be directly compared to ours though, because they used much thinner active layers and tiny active areas compared to the order of m^2 routinely characterized using the R2R technique.[1] Spin coating is also different from doctor blading and R2R coating in that the shear experienced by the liquid is constant during drying, and that the final states are not in thermodynamic equilibrium because material is removed throughout the drying process.

Often, blends that work well in spin coating does not function equally well when applied in R2R coating. Therefore, in order to make comparisons of the morphologies possible and understand the kinetics of R2R coated films specifically, the same kind of detailed characterization used on the more well-known processing techniques have to be applied directly to roll coated films. This study focuses on the active layer and the electrode layers are not included in the R2R X-ray characterization, because the nano-structured electrodes consisting of heavy elements would mask the weak signals from the crystallizing polymer. It is consequently not possible to manufacture solar cells from the exact same coated films. Therefore, we chose a widely used material blend because it is already well-documented as functioning R2R coated solar cells[15,16] and also to enhance the comparability of the study, although the previously mentioned differences in temperatures, concentrations and coating techniques still means that direct comparisons should be done carefully. The limited intensity of our

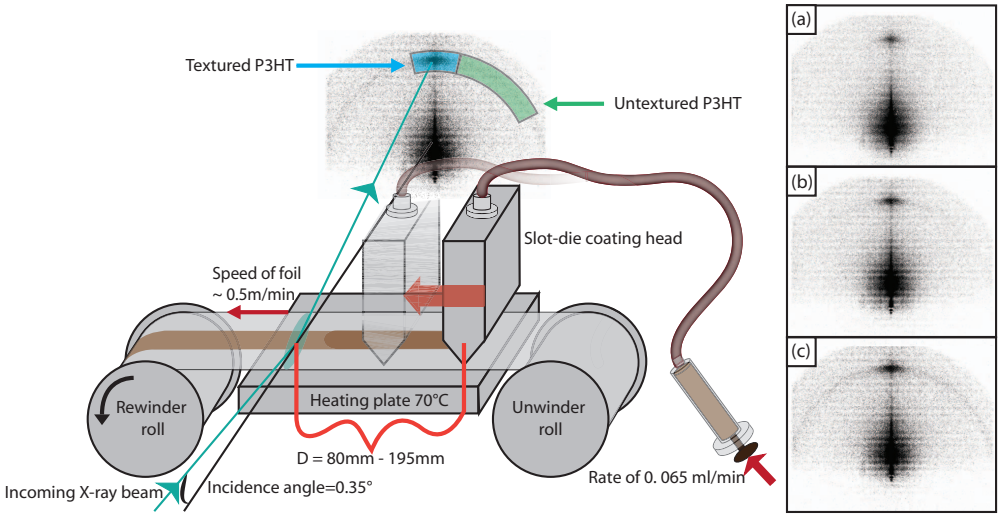

FIG. 1. Here a schematic of the SAXS roll coater is shown to the left, with 3 examples of measurements on the right at distances from the coating head of a) 120 mm, b) 195 mm and c) re-rolled in dry condition, corresponding to 14 s, 23 s and 1 h drying time, respectively. The X-ray beam originates at a rotating anode and enters an evacuated flight tube after hitting the film before encountering the detector 1 m further downstream. Using a syringe the polymer/fullerene mix is pumped through the coating head with a constant rate, while the rewinder pulls the foil from the unwinder, thereby depositing a film of the mixture on the foil.

laboratory X-ray source prohibits direct observation of the drying in one specific point of the film, but by sampling from the same state of drying throughout a 30 m long film, moving through the sampling position, we get a statistical average of the structure of the film at a dryness defined by the distance from sampling point to coater head. The results show that the untextured crystallites form very late in the drying process, which was not expected and could possibly be used to improve the total amount of these crystallites.

II. EXPERIMENTAL

Using our SAXS setup for *in situ* measurements required a roll coater unit fitting within the small spatial proportions of the instrument. To reduce the signal to noise ratio due to beam scattering in air, we used a narrow foil for coating in contrast to the wide foils used in standard coating procedures as described in the literature.[17] The narrow web resulted in a significant movement in the cross-web direction, caused by resistance from the surface of the hotplate and the setup was therefore modified with rolls with edge guides enabling a good control of the foil movement. The solar cell was printed on flexible substrate (PET-foil), by rolling the foil from an unwinder roll to a rewinder roll, as illustrated in Fig. 1. A motor rotated the rewinder roll, thereby moving the foil from the unmotorized unwinder to the rewinder, while a film of the active material was coated onto the moving foil using a slot-die coating head. The speed of the foil was about 0.5 m min^{-1}. The slot-die coating head is two pieces of metal with a narrow gap between them where the polymer-fullerene solution is pumped out through a narrow slot onto the film.[18,19] At the shallow X-ray incidence angle, close to the critical angle for total reflection, even a very slight tilt of the foil gives strong reflections of the incident beam, saturating the detector. To ensure a stable, wobble-free movement, a brake was applied to the unwinder roll to increase the web tension such that the film was pulled tight between the rolls. The whole roller apparatus was mounted on a cradle enabling precise control of incidence angle and height. This completed setup enabled excellent control over web position, web orientation and tension, coating position, drying front, X-ray beam position and X-ray footprint on the moving foil.

By changing the distance between the coating head and the point where the X-rays illuminate the film from 80 mm to 195 mm from the point of coating we achieved measurements for different

stages in the drying process, corresponding to drying times of 10-25 s. The investigated drying times were limited by the physical length of the heating plate which defined the coating surface. At 70°C the film dries quite fast, the drying front being only about 5 cm from the coating head, therefore the limits of the setup meant that we could only study the development after the drying front, and when referring to measurements on "wet" film, this indicates the area right after the drying front. The experiment was performed under normal atmospheric conditions because the aim is to investigate the kinetics of the structure formation in the film under the same conditions as those for large-scale production.

The polymer-fullerene mix used was a 1:1 w/w mixture of poly(3-hexylthiophene) (P3HT) and poly(3-hexylth-iophene):(6,6)-phenyl-C61-butyric acid methyl ester (PCBM) prepared in a chlorobenzene solution, (30:30 mg/mL). 98% regioregular P3HT was obtained from BASF, Sepiolid P200; PCBM from Solenne BV and chlorobenzene from Sigma Aldrich, all of analytical grade. The 13 mm wide active layer was coated with a pumping rate of 0.065 ml/min, a temperature of the heating plate of 70°C and the speed of the substrate of about 0.5 m/min corresponding to a wet layer thickness of 10 μm which gave an average dry thickness of the film of 480 nm. The scattering patterns were recorded at an incidence angle of 0.35° with Cu-Kα radiation ($\lambda = 1.5418$ Å) generated from a rotating copper anode operated at 40 kV/40 mA, focused by a 2D multilayer optic and collimated by 3 pinholes, giving an intensity of the beam at the sample position of $\sim 10^7$ s^{-1}. With a beam diameter of 1 mm and the very shallow incoming angle of 0.35°, the beam footprint on the sample is much wider (16 cm) than the width of the active layer film, ensuring that the active layer is at all times illuminated. Every experiment had two stages – first the *in situ* measurement was performed, while coating the layer. Afterwards, the foil was rolled back to the starting position and a measurement on the now dry foil was performed, giving about an hour between the wet and dry measurements.

Because each measurement consisted of coating a length of foil, the amount of scattering data was limited by the possible length of foil and the speed of the coating, as well as the intensity of the X-ray source. The speed was chosen both based on specific requirements for the thickness of the active layer, and simple physical limits set by how the materials wet the foil surface. If the speed is too slow, the film becomes uneven, and if the speed is too high, the material might not evenly wet the surface, creating an effect similar to water paint on a plastic surface. We chose the slowest possible speed with which we could achieve the correct layer thickness, and combined this with the longest possible foil to get as much scattering as possible per experiment. The scattering was then recorded 100 s at a time consecutively for the full length of the foil. These files were then added together to give the data illustrated in Fig. 1.

III. RESULTS AND DISCUSSION

The measurement described above was performed for 4 different distances between coating head and illumination point, corresponding to four different drying times. Finally, two of the four measurements were omitted because reflections from the PET foil and alignment of the setup hindered quantitative comparison with the other measurements. The observed trends were however qualitatively confirmed. The measurements with drying times of 14 s and 23 s are shown in Fig. 1 together with a measurement of one of the dry films for comparison. As expected, a reflection at q $\sim$ 0.39 Å^{-1} ($|\mathbf{q}| = 4 \cdot \pi \cdot \sin\theta / \lambda$, where θ is half the scattering angle) attributed to the *100* lamellar stacking for textured P3HT is observed in all measurements, represented by the blue ring segment in the setup rendering in Fig. 1. The position of the peak directly above the beam center shows that the polymer orients in the edge-on orientation.[10] In our experiment we only see the first order reflection from P3HT, higher orders are outside the range of the detector, and so is diffraction from possible PCBM crystallites. The measurement at 80 mm from the coating head also showed the Bragg peak indicating that the crystallization already started before 9 seconds of drying. In the *ex situ* measurement performed after about 1 h of drying ((c) in Fig. 1), we observed the ring of scattering from untextured crystallites of P3HT, represented by the green ring segment in Fig. 1. The ring was also observed very weakly in the driest of the *in situ* measurements. This means that even after most of the solvent appears to have evaporated, the formation of untextured crystallites, one of the two main crystallographic developments, is still taking place. This could mean that the

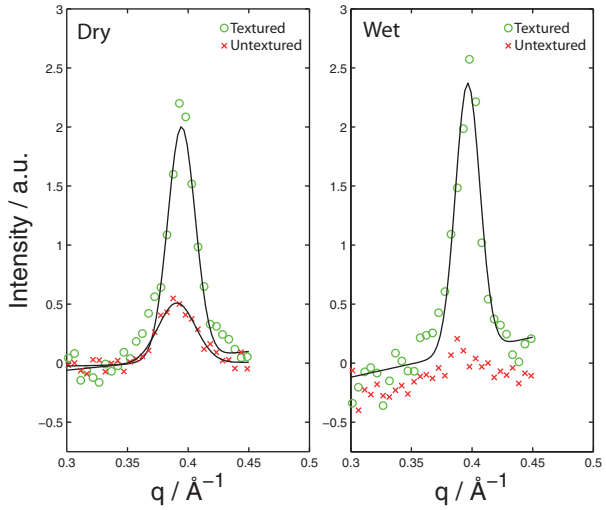

FIG. 2. The integrated peaks for the textured peak and the untextured ring in the dry film (left) and the driest of the wet films (23 s drying time) (right). Solid lines are fits of a Gaussian function and a linear background.

evaporation of the solvent has less impact on this part of the morphology development, which would be interesting to investigate further. To improve signal to noise ratio, the 2D scattering images were integrated through a ring segment of 40 degrees centered on the peak, as illustrated in Fig. 1. Similarly, the integration of intensity for the untextured scattering was carried out in two ring segments on each side of the textured peak to exclude scattering from the textured crystallites. An example of the obtained peaks from both wet and dry material is shown in Fig. 2. From the peak positions we found the average lamellar packing distance d_{100} ~16.0 Å, consistent with previous SAXS studies of P3HT.[9,20,21] The average lamellar packing distance for the untextured crystallites were a little larger(16.1 Å), contrary to earlier findings.[9] In the present study, the coated film was at all times kept at 70°C, whereas the results reported by Böttiger *et al.*[9] were obtained at room temperature. It may be speculated that untextured and textured crystallites exhibit different thermal expansion, but the exact mechanism for the difference is still being investigated, and underlines the need for further studies of the kinetics of roll-coated films. The size of untextured crystallites was smaller (around 16 nm) than the size of textured crystallites, determined to be 22 nm from the Scherrer equation.[22]

The reason we differentiate so sharply between textured and untextured crystallites is that in our measurements the azimuthal width of the Bragg peak coming from the textured crystallites only seems to increase slightly with drying time, whereas a continuous ring with the same average intensity dependence on angle appears superimposed on the peak. This is different from most other studies where an increase in the width of the peak is observed indicating a gradual increase in orientational spread. Our results show that the untextured crystals form independently, instead of gradually building up and becoming more randomly oriented.

The integrated intensity in the peak obtained by summing up the intensity in the ring segments shown in Fig. 1 is a relative measure of the amount of crystallinity. The peak from textured P3HT increases in intensity as the film dries, and the ring of scattering from untextured P3HT crystallites is very weak/nonexistent until the film is dry. This indicates that the textured crystals build up from the interfaces, while there is very limited formation of untextured crystallites in the wet material. As the drying represents an increase in concentration, a probable explanation is that the formation of crystals without a facilitating interface is dependent on the concentration of the polymer. If the P3HT begins crystallization at the interfaces, it means that the concentration of PCBM rises continuously with the crystallization of P3HT because the P3HT crystals contain very little PCBM.[23] This could explain the late formation of untextured crystallites of P3HT since their formation depends on the concentration of P3HT being higher than a certain amount, as reported earlier.[9] This gradual increase in PCBM concentration could result in a gradual change of the morphology resulting from the changing concentration relationship, possibly creating layers of larger vs. smaller PCBM

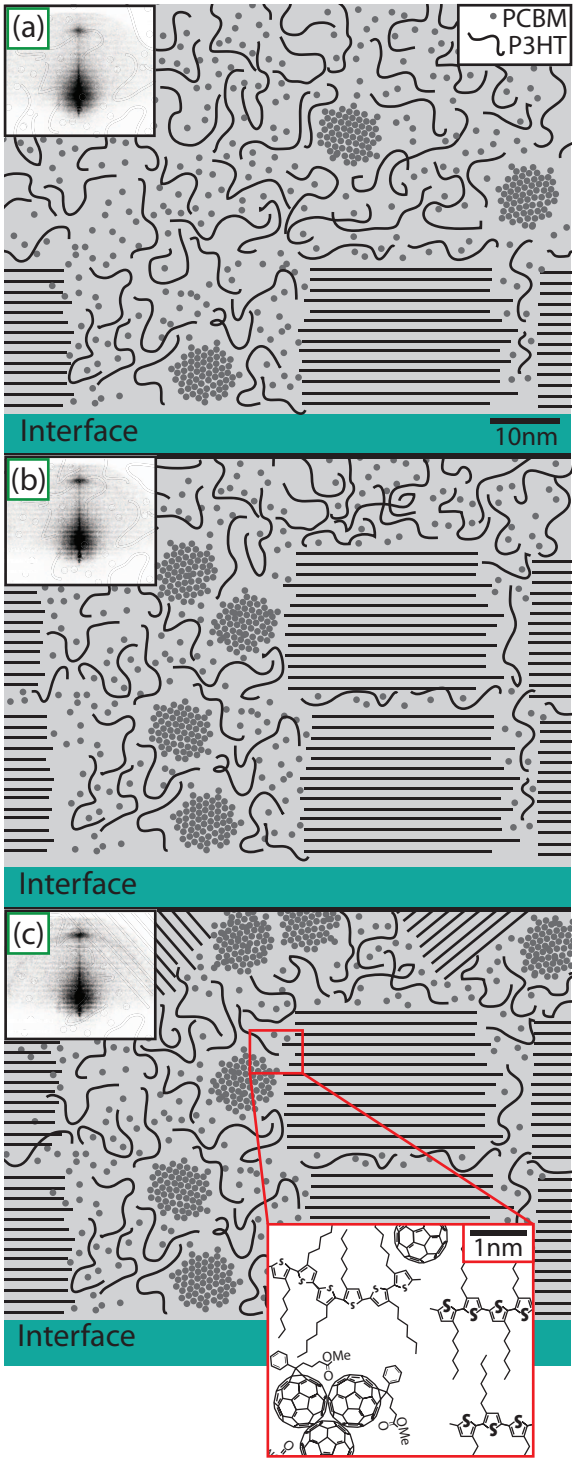

FIG. 3. This is a schematic of the way we propose the crystallization happens. a) First the crystallization begins at the interfaces, then at b) as the solvent evaporates more textured crystallites form and finally at c) the film is dry and we observe untextured crystallites.

crystallites depending on the distance from the interfaces. A direct investigation of the crystal structure dependence on depth is not possible with the current setup, but combining our *in situ* roll coater with techniques such as the ones used in ref. [24–26] would make it possible to determine whether the crystallization originates at both interfaces, and if not, which one that is preferred.

IV. OUTLOOK AND CONCLUSIONS

In conclusion, the SAXS measurements showed crystallization of P3HT, both textured edge-on and untextured during *in situ* roll-to-roll coating. Studying the drying *in situ* showed that textured crystallites are formed earlier than 9 s after deposition of the material, but untextured crystallites takes longer to form, and appear not to form before nearly all solvent has evaporated.

Based on our results, we propose that the drying process comprise a textured crystallization beginning at either one or both interfaces, and a late formation of untextured crystallites in the bulk material when the concentration of P3HT is high enough, after sufficient evaporation of solvent. The process is described in Fig. 3. This would create layers with different final morphology caused by the concentration gradient stemming from P3HT crystallization beginning at the interfaces. This is also known to take place during spin coating,[27] although the mechanisms responsible are probably different. The relationship to concentration is based on a previous study,[9] where the concentration of the coated material was varied by adding an increasing amount of solvent. They found a lower boundary of 1:2 for the concentration of P3HT:PCBM under which there was no formation of untextured crystallites. In contrast to the *in situ* studies performed on spin coating,[28] we observed scattering from the untextured crystallites that is independent of the scattering from the textured crystallites. This suggests that the formation of untextured crystallites is governed by different processes in R2R coating than spin coating.

With this experiment we have shown that *in situ* X-ray scattering is possible even on moving foils, enabling *in situ* X-ray studies of R2R coated materials. This is the first step towards developing a comprehensive understanding of how the morphology in these layers is developed. Combined with studies of concentration ratios, solvents, drying temperatures and other processing parameters, this will give insight into the general behavior of these polymers when they dry and how they form the observed morphologies.

ACKNOWLEDGMENTS

This work has been supported by the Danish National Research Foundation, the Danish Council for Strategic Research (project WAPART, j.no. 11-116380), the Danish Ministry of Science, Innovation and Higher Education under a Sapere Aude Top Scientist grant (no. DFF – 1335-00037A), an Elite Scientist grant (no. 11-116028), the European Commission as part of the Framework 7 ICT 2009 collaborative project ROTROT (grant no. 288565) and the European Research Infrastructure (SOPHIA).

[1] J. Alstrup, M. Jørgensen, A. J. Medford, and F. C. Krebs, ACS Appl. Mater. Interfaces **2**, 2819 (2010).
[2] J. Halls, C. Walsh, N. Greenham, E. Marseglia, R. H. Friend, S. Moratti, and A. Holmes, Nature **376**, 498 (1995).
[3] G. Yu and A. J. Heeger, J. Appl. Phys. **78**, 4510 (1995).
[4] G. Yu, J. Gao, J. C. Hummelen, F. Wudl, and A. J. Heeger, Science **270**, 1789 (1995).
[5] C. Deibel and V. Dyakonov, Reports Prog. Phys. **73**, 096401 (2010).
[6] P. Müller-Buschbaum, Adv. Mater. 1521 (2014).
[7] S. Westenhoff, I. Howard, and R. Friend, Phys. Rev. Lett. **101**, 016102 (2008).
[8] M. A. Ruderer, R. Meier, L. Porcar, R. Cubitt, and P. Müller-Buschbaum, J. Phys. Chem. Lett. **5**, 683 (2012).
[9] A. P. L. Böttiger, M. Jørgensen, A. Menzel, F. C. Krebs, and J. W. Andreasen, J. Mater. Chem. **22**, 22501 (2012).
[10] H. Sirringhaus, P. J. Brown, and R. H. Friend, Nature **401**, 685 (1999).
[11] A. Salleo, T. W. Chen, A. R. Völkel, and R. a. Street, Phys. Rev. B **70**, 115311 (2004).
[12] D. Chen, A. Nakahara, D. Wei, D. Nordlund, and T. P. Russell, Nano Lett. **11**, 561 (2011).
[13] M. Sanyal, B. Schmidt-Hansberg, M. F. G. Klein, A. Colsmann, C. Munuera, A. Vorobiev, U. Lemmer, W. Schabel, H. Dosch, and E. Barrena, Adv. Energy Mater. **1**, 363 (2011).
[14] K. W. Chou, B. Yan, R. Li, E. Q. Li, K. Zhao, D. H. Anjum, S. Alvarez, R. Gassaway, A. Biocca, S. T. Thoroddsen, A. Hexemer, and A. Amassian, Adv. Mater. **25**, 1923 (2013).
[15] J. E. Carlé, T. R. Andersen, M. Helgesen, E. Bundgaard, M. Jørgensen, J. E. Carle, and F. C. Krebs, Sol. Energy Mater. Sol. Cells **108**, 126 (2013).
[16] J. E. Carlé, M. Helgesen, M. V. Madsen, E. Bundgaard, and F. C. Krebs, J. Mater. Chem. C **2**, 1290 (2014).
[17] H. F. Dam and F. C. Krebs, Sol. Energy Mater. Sol. Cells **97**, 191 (2012).
[18] F. C. Krebs, Sol. Energy Mater. Sol. Cells **93**, 465 (2009).
[19] F. C. Krebs, Sol. Energy Mater. Sol. Cells **93**, 394 (2009).
[20] B. Schmidt-Hansberg, M. Sanyal, M. F. G. Klein, M. Pfaff, N. Schnabel, S. Jaiser, A. Vorobiev, E. Müller, A. Colsmann, P. Scharfer, D. Gerthsen, U. Lemmer, E. Barrena, and W. Schabel, ACS Nano **5**, 8579 (2011).

[21] F. Liu, Y. Gu, J. W. Jung, W. H. Jo, and T. P. Russell, J. Polym. Sci. Part B Polym. Phys. **50**, 1018 (2012).
[22] P. Scherrer, Nachrichten von Der Gesellschaft Der Wissenschaften Zu Göttingen (1918).
[23] B. A. Collins, E. Gann, L. Guignard, X. He, C. R. McNeill, and H. Ade, J. Phys. Chem. Lett. **1**, 3160 (2010).
[24] M. V. Madsen, K. O. Sylvester-Hvid, B. Dastmalchi, K. Hingerl, K. Norrman, T. Tromholt, M. Manceau, D. Angmo, and F. C. Krebs, J. Phys. Chem. C **115**, 10817 (2011).
[25] D. S. Germack, C. K. Chan, R. J. Kline, D. a. Fischer, D. J. Gundlach, M. F. Toney, L. J. Richter, and D. M. DeLongchamp, Macromolecules **43**, 3828 (2010).
[26] C. J. Schaffer, C. M. Palumbiny, M. A. Niedermeier, C. Jendrzejewski, G. Santoro, S. V. Roth, and P. Müller-Buschbaum, Adv. Mater. **25**, 6760 (2013).
[27] K. Norrman, A. Ghanbari-Siahkali, and N. B. Larsen, Annu. Reports Sect. "C" Physical Chem. **101**, 174 (2005).
[28] K. W. Chou, B. Yan, R. Li, E. Q. Li, K. Zhao, D. H. Anjum, S. Alvarez, R. Gassaway, A. Biocca, S. T. Thoroddsen, A. Hexemer, and A. Amassian, Adv. Mater. **25**, 1923 (2013).